MORPHOLOGY AND INTERNAL STRUCTURE OF ROCKSLIDES AND ROCK AVALANCHES: GROUNDS AND CONSTRAINTS FOR THEIR MODELLING

A. STROM[1]
Institute of the Geospheres Dynamics, Russian Academy of Sciences, Leninskiy Avenue, 38-1, 119334, Moscow, Russia

Abstract

Massive rock slope failures and subsequent rapid motion of huge masses of debris is a complex process. Data required for its understanding and numerical modelling can be derived from detailed study of the morphology and internal structures of rockslide source zones and deposits. Proposed model to explain their peculiarities must not contradict any of the observable phenomena, which should be regarded as constraints with which to check a model's reliability. To develop reliable models for the formation and motion of rockslides and rock avalanches we must take into account the whole assemblage of morphological, structural and depositional features typical of them. Proceeding from case-by-case analysis to a comprehensive synthesis of the whole phenomenon requires systematisation and classification of all of the observable features typical of numerous rockslides and rock avalanches. Classification criteria and principles of data analysis and classification that allow selection of different types and genetic sequences of the phenomena in question are presented and discussed. They are illustrated by case studies from Central Asia, the Caucasus and some other regions.

1. Introduction

Massive rock slope failures and subsequent rapid motion of large-scale rockslides is a complex process that still remains a mystery in many respects. Very few of them have been witnessed, and even fewer watched by experts from positions of safety, and so able to analyse them objectively. In studying prehistoric rockslides, we usually cannot reconstruct with confidence the important pre-failure and failure conditions: was it in the wet or dry season?, did an earthquake occur or not?, etc. Therefore, most of the information that can be used to explain rockslide formation and rapid motion and to develop mechanical models must be derived from detailed study of the morphology and internal structure of the source zone and the rockslide deposits. The explanation of their peculiarities by any proposed model must not contradict any of the observable phenomena.

This paper focuses on the processes of debris motion and deposition; causes of slope failure are outside its limits. I would only like to dwell on the role of strong earth-

[1] *E-mail*: a.strom@g23.relcom.ru

S.G. Evans et al. (eds.), Landslides from Massive Rock Slope Failure, 305–326.

quakes, which are often considered a causative factor, not only of slope failure itself, but also of long runout. It was proposed in particular, that rock avalanche can move during strong earthquake as if on a vibrating table [62]. But intense shaking lasts only for tens of seconds even in the strongest earthquakes [52]. During this short interval, a huge rock mass must first separate from the main massif, accelerate down-slope, and only then form a rock avalanche. Obviously it will take much more time. The true role of seismic shaking in rock-avalanche formation can be shown by the July 23, 1988 Tsambagarav earthquake in Mongolian Altai (M 6.4). The earthquake itself formed only a large fissure on the slope, then, 13 days later, a rock-ice avalanche 6 Mm^3 in volume descended from the 320-m high scar and moved 5 km along Zuslan Creek [4]. This shows that long runout is not a consequence of the seismic shaking itself. Moreover, the morphological similarity of earthquake-induced rockslides and rockslides not associated with earthquakes indicates that their peculiarities are determined mainly by the processes acting during their motion, and not by their causes.

An outstanding feature of rockslides that convert into long runout rock avalanches is their abnormal mobility and its increase with increasing volume. It has always attracted attention, and numerous models have been proposed to explain it [5, 8, 9, 10, 13, 17, 18, 19, 30, 33, 34, 35, 36, 39, 42, 44, 45, 48, 50, 56, 58, 59, 67, 68, etc.]. However, high mobility is only one characteristic of rockslides. Ignoring other features can lead to hypotheses that are invalid on their physical grounds, though giving reliable assessment of debris runout, as demonstrated for example by Erismann [14]. Thus, to develop a realistic model(s) of the formation and motion of rockslides and rock avalanches, we must take into account not only the long runout, but also as many other of their peculiarities as well. Ideally, the whole assemblage of morphological, structural and depositional features should be explained within the framework of any proposed model, and the observable phenomena should be regarded as constraints with which to check a model's reliability.

Some peculiarities of rockslide morphology, debris distribution and properties that have been used for theoretical analysis as universal ones may reflect only rare, or particular cases (see, for example, schemes, presented by Kilburn & Sørensen [34, figure 3] and Legros [39, figure 1]). It also appears that not all features that can shed light on rockslide mechanisms can be observed and studied at one rockslide. Depending on circumstances, some rockslides preserve excellent surface morphology, but almost nothing can be said about the internal structure of their deposits and vice versa. Thus, to proceed from case-by-case analysis to a comprehensive synthesis of the complete phenomenon, we must systematise and classify all of the observable features typical of many rockslides and rock avalanches. It requires compilation of worldwide database, that should include not only their geometric parameters such as volume and H/L ratio, but also a complete morphological and lithologic description of each rockslide. Such systematisation was performed, for example, by Shaller [56] and by Nicoletti & Sorriso-Valvo [47]. Now, more than 10 years later, when numerous new data on large rockslides and rock avalanches in different parts of the world have been collected [1, 23 - 25, 26 - 29], and several new large data bases compiled [see, for example, 15, 39] it seems that it is time to revisit the issue. Of course it is extremely difficult to compile a uniform worldwide database, since different descriptions often focus on the specific

features that attracted an authors' attention. Even the terminology in this field of earth science is not standardised. Nevertheless such compilation seems to be important milestone. In this article, I would like to describe some principles of data analysis and classification, that allow selection of different types and genetic sequences in rockslides and rock avalanches. These should be considered to be grounds and constraints for modelling rockslides and rock avalanches.

2. Principles of Data Classification and Systematisation

The first step in this analysis is to identify features that are typical of rockslides and rock avalanches, and independent of the geology and geomorphology of their sites. These features can be considered to be universal patterns reflecting the general processes of rockslide formation and motion. Analysis of field data from the Tien Shan, Pamirs, Caucasus, Alps and descriptions of similar phenomena elsewhere allow such universal features to be selected. These are:

1) The increase in debris mobility (runout and apron dimensions) with increase of rockslide volume;
2) The comminution of rock mass in the internal/lower parts of rockslide deposits and the presence of much coarser material in their external and upper parts;
3) The lack of mixing of different lithologies from the slope failure to the resultant debris deposit.

The next step is to deduce the geological and geomorphic conditions that lead to the different rockslide debris morphologies and internal structures. These can be used as criteria of classify massive rock slope failures. Based on my personal experience and literature review, I would like to suggest several classification criteria of rockslides and rock avalanches:

1) Conditions of initial sliding (initial slope failure);
2) Relations between the initial (in the massif) and final (in the rockslide deposits) rock sequence;
3) The spatial distribution of the deposits, comparing amounts of debris that came to rest in their distal and proximal parts and characteristics of the boundaries between these parts.
4) Width-to-length ratio of the debris apron. Although this criterion applies mainly to unconfined rock avalanches, it also can be used to classify rockslides formed in rugged topography;
5) Micro-relief of the rockslide and rock avalanche deposits.

The third proposed stage is to identify rockslides and rock avalanches showing gradations in morphological or structural parameters that can be considered to represent consecutive stages of some process. We can either look for different extents of development of the same feature at several case studies (extent of runup, for example [see 29, figure 14]), or analyse gradual or abrupt change in any morphological or depositional parameter within one rockslide/rock avalanche body, that might indicate transformation of some mechanical processes during emplacement. The latter can be illustrated by

extent of debris comminution in different parts of rockslide deposits, or by micro-morphological patterns on a rock-avalanche surface.

3. Universal Patterns of Rockslides and Rock Avalanches

The *increase of runout* with increasing volume of failure was first recognised by Heim [22] and later shown statistically by Sheidegger [58], Hsü [30], Shaller [56], Li Tianchi [40], Sassa et al. [53], Legros [39]. Estimations of H/L ratio versus rockslide volume used in such analyses are not always well posed. Sometimes in the same plot we can see parameters of the Blackhawk and Sherman Glacier rock avalanches that spread over unconfined plains, grouped with the Elm and Khait rock avalanches that moved ahead along relatively narrow valleys (channelled type according to Shaller [56]), and also with the Usoi or Köfels rockslides that stopped when they struck the opposite slope of the valley. Shaller divided his database in several groups using the state of confinement, and found that channeling and division of the debris into several separate lobes had no significant effects on the runout [56, p. 73]. The opposite conclusion was reached by Nicoletti & Sorriso-Valvo [47] using a statistical analysis of a smaller database. They found that channeling of debris supported long runout. Shaller used H/L ratio as a mobility measure, while Nicoletti & Sorriso-Valvo used runout length (L) for the same purpose. Such controversy shows the necessity for compilation of more representative database for such studies.

The controversy also demonstrates the importance of selecting the parameter to measure runout, and parameters with which it should be correlated. A comprehensive analysis was done by Legros [39] who showed that H/L ratio (apparent coefficient of friction or 'fahrböschung'), first used by Heim [22] and since then by many other authors, has no physical meaning. The translation of the centre of mass is more physically sound, but it is difficult to estimate it for several reasons. First, its initial and final positions of the centre of mass are often poorly known, and, second, its translation may not adequately reflect the process of debris motion except in the case of the debris distribution described below as ‘primary’ [65]. In other cases when only some portion of the debris has been involved in avalanche-like motion, use of this parameter may lead to erroneous conclusions.

Another pattern typical of the majority of large rockslides is *the intensive crushing of lower/internal parts of rockslide deposits* (sometime up to a sandy engineering soil) and the presence of a much coarser material at their upper/external parts (Figure 1). The latter is composed of large angular boulders, and sometimes of huge fractured blocks of displaced bedrock with only a small content of fines.

For both zones, a common pattern is the presence of jigsaw-puzzle structure where there are blocks much bigger than individual fragments, in which the latter are separated from each other, but retain their initial mutual positions. The significant difference in the extent of debris crushing between the zones indicates different style of destruction. This is typical of rockslides that form high natural dams in river gorges such as the Köfels and La Madeleine rockslides in the Alps [13, 7], the Kokomeren, Djashilkul, Bashi-Djaya [1, 63, 66], recently breached Yashinkul [51] and Issyk (E.I. Gaspirovich, Personal Communication, 1995) rockslides in the Tien Shan, numerous rockslide dams in the Karakoram [28, 29], the Lettopalena rockslide in the Appenines [54], the Upper Mizur and Lower Sadon rockslides in the Northern Caucasus. A generally similar grain

size distribution was observed at Flims [55, 68], although at this event, the different manifestation of debris comminution may be due to peculiarity of the sliding mechanism (described below).

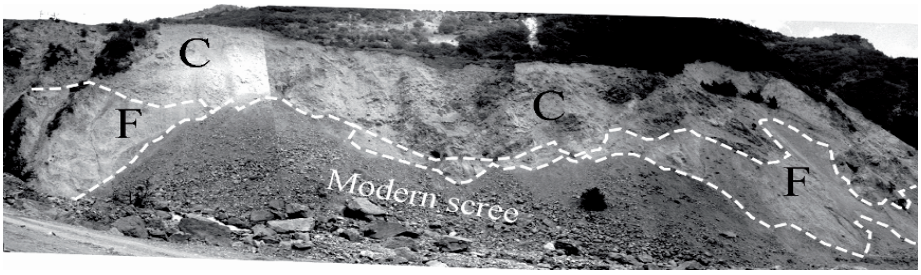

Figure 1. Panorama of the Lower Sadon rockslide (42.85º N, 74.08º E, Northern Osetia, Great Caucasus). Distinct zones are composed of fine-grained (F) and coarse (C) material. Outcrop is 50-70 m high.

The causes of the intensive debris comminution, and the creation of different facies are not yet clear. Some authors [13, 28] attribute it to collision against topographic obstacles (Hewitt wrote: "Topographic blocking constrains cataclastic processes in rock avalanches and creates distinctive facies at depth" [28, p. 80]). But the same features are seen in rock avalanches that moved across unconfined topography as well, such as at Blackhawk [32, 61], "Ancient" and Inylchek rock avalanches [1, 63, 64]. Thus it seems that intensive comminution and formation of different facies in rockslide deposits are peculiarities of large-scale rock failures, irrespective of the topography of the transition and deposition zones. On the other hand, in the Karakoram, (K. Hewitt, Personal Communication, 2002) has observed that the extent of comminution in the lower parts of very thick rockslide deposits is higher than in 'ordinary' events. This also is supported by evidence of very intensive shattering in the lower part of the Kokomeren rockslide [66], which is comparable with the giant Karakoram events.

A further peculiarity of rockslide deposits, seen in numerous cases worldwide and, thus, considered a universal feature, is the *absence of mixing* of different lithologies involved in the collapse, in the resultant debris. At the local scale this is expressed as jigsaw-puzzle structure, but the same lithology may persist sometimes through larger portions of the debris, far larger than the puzzle blocks. As with many other typical features of rockslides, it was first described by Heim [22]. Although (as it analysed below), retention of the initial stratigraphy does not exhaust the observable relationships between rock types involved in slope failure, lack of mixing, and the presence of jigsaw-puzzle structure demonstrate that motion of large portions of debris was laminar, without significant relative internal mutual displacement of the separate fragments.

Processes that cause above-mentioned effects are fundamental to the formation or rockslides and rock avalanches.

4. Differences in Debris Morphology and Internal Structure – Criteria of Classification

Comparison of similarities and differences between numerous rockslides and rock avalanches in a large verity of geological and geomorphic environments, leads to a better understanding of the controls governing their processes of formation and motion.

4.1. CONDITIONS OF INITIAL SLIDING

Significant differences in a rockslide's internal structure and displacement mechanism may be caused by different conditions of initial sliding. Many types and subtypes can be identified using this criterion, but I will focus here on two of them: failures along bedding planes and failures across bedding. Bedding-plane failures occur if huge units of strata slide along inclined bedding planes, usually on limbs of large folds. They can be contrasted with rockslides of the across-bedding type, where sliding surfaces cut boundaries between geological units. Failures in unstratified rocks, such as some plutonic igneous rocks, generally can be related to the across-bedding type, since in most cases there are no regular systems of pre-existing surfaces along which sliding occur. The bedding-plane type (Figure 2-A, B) can be considered to be a special case of translation rockslides, whereas both translation and rotation may occur along sliding surfaces in the across-bedding rockslides. Classical examples of the bedding-plane rockslides are Flims in the Swiss Alps [2, 55]; Seimareh in Zagros, Iran [20, 60, 68]; and Avalanche Lake in the Mackenzie Mountains, Canada [11, 16].

The numerous large rockslides in Tien Shan [1, 63, 66], Pamirs [57], and on the southern slopes of the Rocky Range of Northern Caucasus are typical across-bedding events (Figure 2-C). This type of rockslides also can be illustrated with the 'rockfall-avalanches' on the Sawtooth Ridge in Montana described by Murge [46]. He contrasts 'rockfall-avalanches' with 'rockslide-avalanches', which exactly correspond to the above 'bedding-plane' type. But I would like to note that most of large-scale massive slope failures with very rare exceptions originate as 'slides', and not 'falls'. That is why I prefer to use the term 'rockslide" rather than 'rockfall'.

In some failures, the upper part of the initial sliding surface crosses geological boundaries while its lower part follows a bedding plane. An example of such a mixed type of slope failure is the giant Beshkiol rockslide in the Naryn River valley [66].

Differences in initial sliding conditions may lead to significant differences in the mechanism of rockslide motion. Rockslides of the bedding-plane type may initially have slid along pre-existing bedding plane failures, with low residual friction, and, therefore, faster acceleration. It may explain ultra-mobility of such events as, for example, the Avalanche Lake rockslide [16]. In this case detached massif can move either as a single block (see figure 2-A) or, as a deck of 'playing-cardd' as proposed by Schneider, Wassmer and Ledésert [55], where each overlying stratum can slip relative to the underlying one, with only a small relative displacement between adjoining strata (see figure 2-B). It would result in a higher speed and longer runout of the uppermost layers. This discrete displacement of rock slabs, generally corresponding to separate layers has created a specific structure in the rockslide debris observed at Flims [55, 68]. According to this model, the distal part of the rockslide body should be composed of units, that originally formed the outer part of the slope. In some cases, however, 'playing card mechanism' can not work. In particular, in the 'bedding-plane' Rockslide Pass rock avalanche in the Mackenzie Mountains there is clear evidence of longer runout of a unit that originally formed a basal part of the sliding mass (the so-called 'Red Rim') [11]. Such a significant difference in mechanism of debris motion might be explained as follows: in the Flims case, the downslope length of the detached massif (3 to 7 km) was much bigger than its thickness (~0.5 km) and, thus, it could only slide along bedding planes. In contrast, at Rockslide Pass, the thickness was of the same order as its length

(about 500 m), and so, when the strength of its lower units was reduced due to rock fragmentation, it could topple backwards and move as an across-bedding event rather than as a bedding plane one.

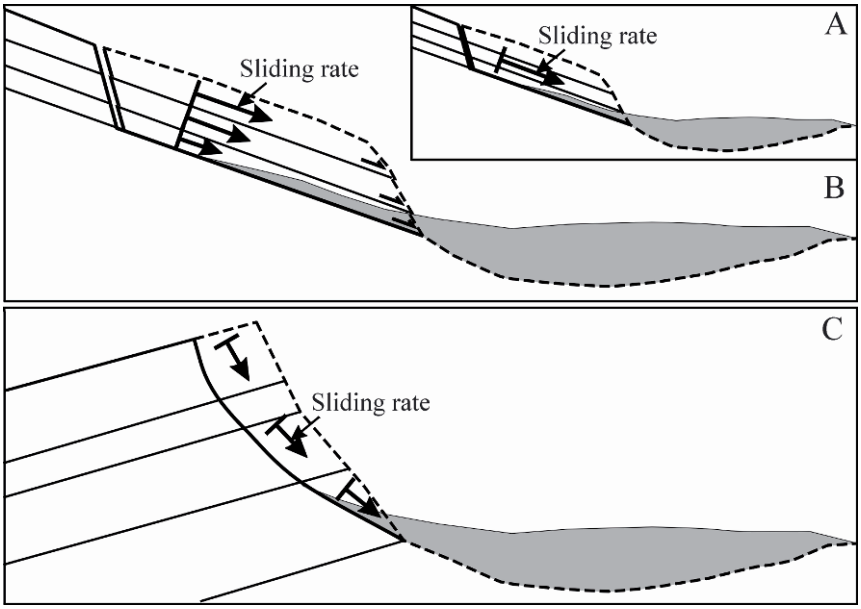

Figure 2. Initial sliding rate distribution in the bedding-plane (A, B) and across-bedding (C) rockslides. A – detached massif starts moving as a single block, B – 'Playing card' model.

The initial motion of the across-bedding rockslides is significantly different from that in bedding-plane failure. Irrespective of if it is a translation along a planar sliding surface or rotation on a cylindrical one, the 'playing-card' mechanism can not work here, since there is no pre-existing system of parallel sliding surfaces. In such a case, rocks that originally lay at the foot of the slope move in front of the sliding mass, being pushed by its main part, which having descended from the higher part of the slope had a higher initial potential energy (see figure 2-C). The distal part works as a 'brake' preventing free acceleration of the following rock mass. Hence, until debris from the upper part of the slope cuts across the moving body and overruns the frontal part (this process is analysed bellow), the speed of the whole rockslide should be similar. In the distal parts of across-bedding rockslide deposits, we often observe debris, which originated from rocks that outcrop at the foot of the scars (Figure 3-A). This corresponds to preservation of the initial stratigraphy and is well illustrated by the Imom rockslide in Pamirs [63] and the Ksurta and Sularta rockslides in Northern Osetia. Similar relationships are observed at Rockslide Pass.

4.2. RELATIONS BETWEEN THE INITIAL AND FINAL ROCK SEQUENCE

Preservation of the original stratigraphy in the resultant deposits first described by Heim [22] does not exhaust the observable relationships between rock types involved in slope

failure. Two main types of rockslide bodies can be identified on the basis of this criterion: those retaining true original stratigraphic relationships between strata and those converted into 'stratified' bodies [63]. The principal difference between these types is shown on Figure 3.

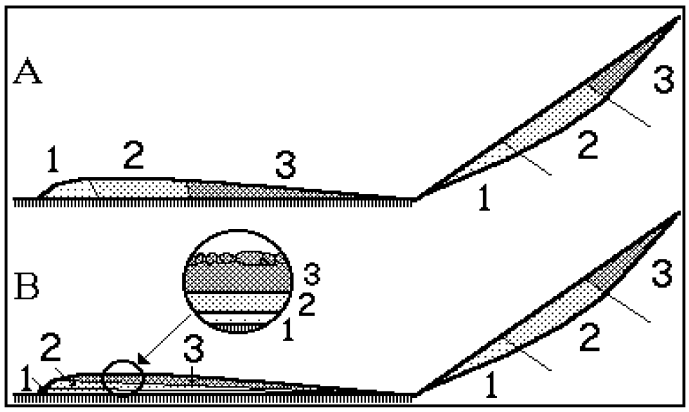

Figure 3. Typical structures of rockslide deposits of the across-bedding type (after [63]). A – with the retained initial sequential order of rock types (Imom, Ksurta, Sularta rockslides); B – converted into a 'stratified' body composed of layers of homogeneous lithology (Kokomeren, Inylchek, Blackhawk rockslides).

In the first case, the sliding mass moves as a flexible sheet, while in the second, the following parts overtake and overlap frontal portions of debris. Analysis of factors that might determine the retention or conversion of rock sequence focuses attention on the shear strength at the sliding interface and inside the moving debris [63]. It should be the ratio of these strengths that governs the formation of 'retained' or 'converted' sequences of lithological units. In the latter, the sequence results from overthrusting of units from the upper parts of slope over those initially resting down-slope, due to shearing along boundaries between different lithological units, which cross the moving debris. Such shearing usually does not occur inside any unit. It suggests that geological boundaries (stratigraphic, plutonic or tectonic) are either zones of weakness, or that the shearing is associated with some difference in rock material properties.

According to Grigorians' model [18] maximum shear stress at the contact of the moving debris and the basement can not exceed the strength of the weaker material. This conclusion could be extended to the extreme shear stress inside moving debris that can not exceed the debris's shear strength. The resistance to debris motion along the base depends on the contact area and on the shear strength of the weaker material. On the other hand, the resistance to shearing of the moving debris along any internal secant surface depends on the latter area and on the debris's dynamic shear strength. Depending on the ratio between basal shear and internal shear resistance, the front of the sliding mass should be either pushed forward (and the initial sequential order of rocks retained, see figure 3-A), or it is overthrust by the following debris to form a 'stratified' body

(see figure 3-B). Judging by the structures in many studied rockslide deposits, such overthrusting can occur a number of times.

If internal stress in the rock avalanche are not high enough for discrete shearing and overthrusting take place, then transverse ridges (folds) develop on the deposit's surface due to longitudinal compression in the moving debris [12, 20, 33, 61]. Such features have been seen on the surface of the multi-layered Blackhawk rockslide, and so it is very likely that the same process can occur in the final stage of rockslide motion after its 'stratification' is complete. Possibly the same process can form the cascade profile typical of rock avalanches in narrow valleys.

4.3. DEBRIS DISTRIBUTION IN ROCKSLIDE DEPOSITS

Another variable pattern in rockslide deposits is the debris distribution between distal and proximal parts. This distribution may be governed by the relief of the slope foot where the initial acceleration ceases and the debris continues its motion under its own momentum. Significantly different debris distributions have been observed in similar-sized rockslides that descended from slopes composed of Palaeozoic granites in the Central Tien Shan. Three main morphological types of rockslides/rock avalanches can be separated by use of these criteria (Figure 4) – primary, secondary and spread [65].

1 – *Primary* rock avalanches are characterised by debris accumulation in their distal parts. An excellent example of this debris distribution is the Seit rock avalanche in the Tien Shan (Figure 5-A) [65], which looks like as if all of its debris 'flowed' downstream through a narrow gorge to form a giant 'drop'. Good examples of similar type of debris distribution when it crossed the valley but runout was confined by opposite slopes are the well-known Köfels rockslide in Tirolean Alps, and Usoi rockslide in Pamirs. These both have prominent lowering at their proximal parts.

2 – Rockslides with a compact body at the foot of collapsed slope, and with a well-defined secondary scar, from which a portion of debris has moved as an avalanche, represent *secondary* rock avalanches (see figure 4). In many cases, the amount of debris involved in the avalanche motion is much bigger that volume of the associated secondary scar. It seems that secondary rock avalanches are ejected from the deposit accumulated at the scars' foot by the mechanism of abrupt momentum transfer when the rockslide collides with an obstacle. Hence, the secondary scar is just an indication of an abrupt change of motion during a two-stage process as illustrated by the Chongsu and Southern Kara-Kungei rock avalanches in Tien Shan (Figure 5-C, D, Figure 6) [65]. Several avalanches that can ascribe to *secondary* type were described by Eisbacher [11] in the Mackenzie Mountains (Nozzle Slide, U-turn Slide). Many subtypes of secondary avalanches can be identified, depending on the direction of secondary motion relative to that of the initial motion (inherited, oblique, or perpendicular), or to portion of debris involved in such failure (compare for example the Chongsu, Southern Kara-Kungey and Kolsay rockslides on figures 5 and 6). The presence of secondary scar is the characteristic feature of this morphological type of rock avalanches.

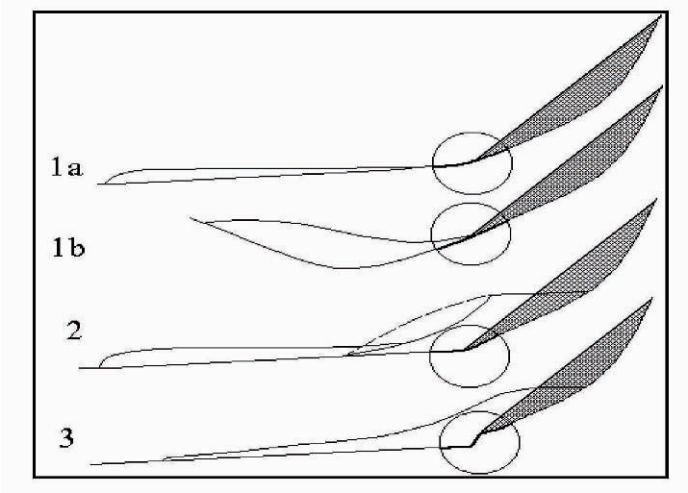

Figure 4. Morphological types of rock avalanches (after [65]). Circles mark part of slope where the initial acceleration ceases and motion continues under momentum.

3 – Rockslides with a compact proximal part and avalanche-like tongues of debris, but without a secondary scar, are classified as *spread* rock avalanches (see figures 4, 5-E, 6). One more peculiarity of this type of motion is the gradual thinning of the rock avalanche deposits from proximal to distal parts. Since they are found in situations where the descending rock mass struck the foot slope at or near to a right angle, it seems that they are produced by squashing of the frontal part of debris under the pressure of the following mass, and this causes its fluidisation.

For example, the famous Elm rock avalanche can be ascribed to the latter type of motion. After its collision with the quarry floor, the rockslide jumped, met the valley floor just at a right angle, and then 'flew' ahead, demonstrating good evidences of fluidisation [21, 31]. Other examples of this type of rock avalanche are the Northern Karakungey event (see figure 5-E) in the Central Tien Shan [65] and the Atdjailau event in the eastern part of this mountain range not far from the Kyrgyz-China border [1].

Both secondary and spread types of rock avalanche are characterised by high proximal thicknesses in their deposits. Many examples from different regions show that these debris distributions are very common, with large portions of debris often resting at the foot of the rockslide scar. That is why I can not agree with Legros who mentioned that high proximal thickness is not typical of landslide deposits [39, p. 304].

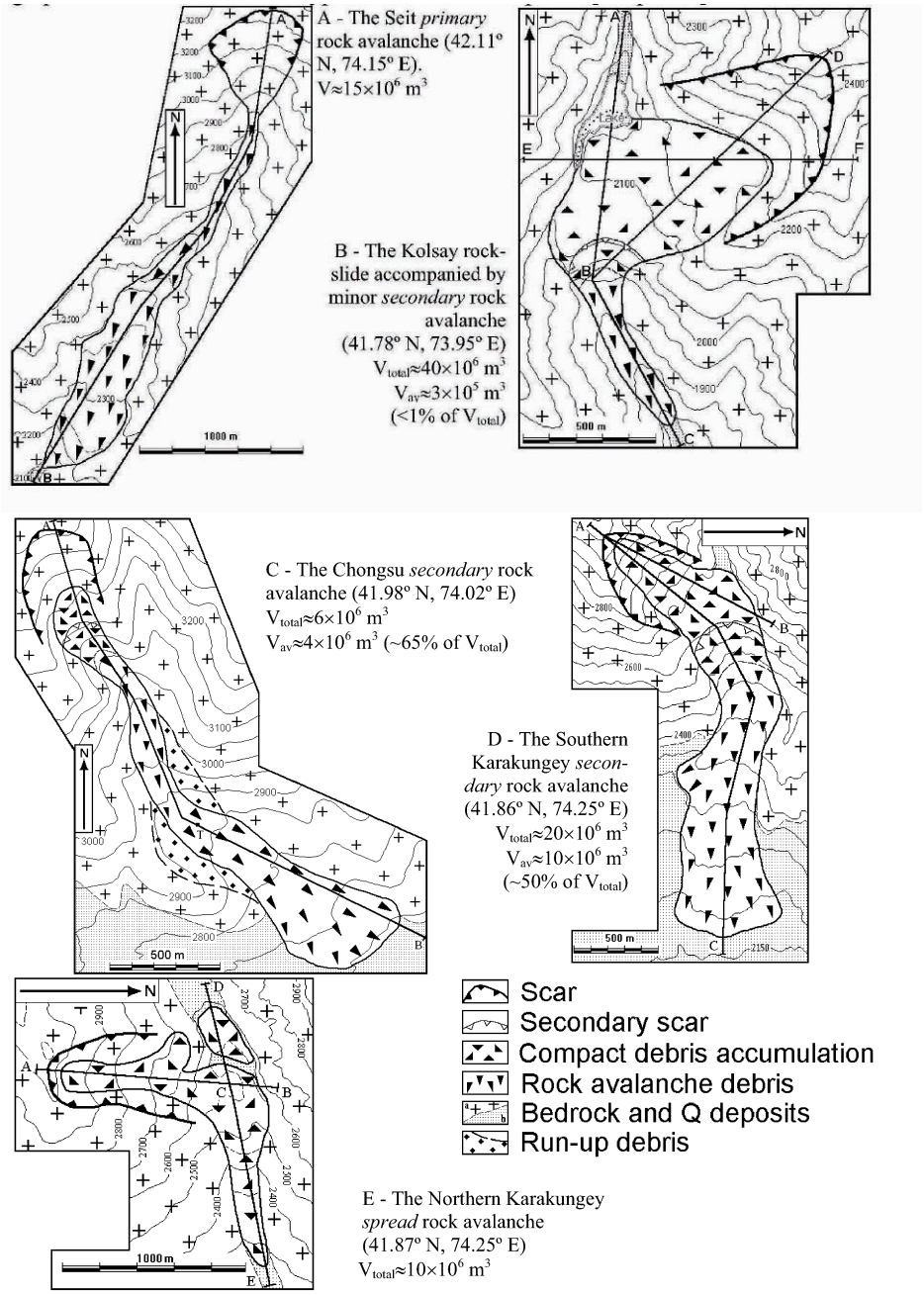

Figure 5. Schematic maps of rock avalanches of different morphological types: Seit – primary, Chongsu, Southern Karakungey and Kolsay – secondary, Northern Karakungey – spread. V_{total} = total volume of collapsed rock mass; V_{av} = volume of debris involved into the avalanche-like motion (after [65], modified).

4.4. WIDTH-LENGTH RATIO OF DEBRIS APRON

Besides the proximal-distal debris distribution described above, rock avalanches can be classified according to the width to length ratio of the debris apron. This classification criterion can be applied, first, to the unconfined events, where motion is governed by basal friction and inter-debris processes, without complications caused by effects of topographic confinement [47, 56]. Monodirectional, fan-shaped and pancake-shaped types of such rock avalanches can be recognised (Figure 7).

With some reservations, rockslides formed in rugged topography also can be classified by this criterion (see [47]). If we analyse the overall morphology of rockslide blockages in deep river valleys, such as described by Hewitt in the Karakoram Himalaya [29], we can see that many of them correspond to the "T-shape" type proposed by Nicoletti and Sorriso-Valvo [47]. At least some such along-valley spreading of rockslide debris can be caused by secondary avalanche formation as at the Karasu Lake rockslide in the Tien Shan (Figure 8). But, at the same time, some rockslides, after collision with the opposite slope of the valley, nevertheless, have steep up- and downstream slopes and, hence, moved generally forward without pronounced lateral spreading. Exemples of these are the Köfels rockslide in the Tyrolean Alps and the Aksu and Djashilkul rockslides in the Tien Shan [1].

Similar differences can be observed in cases when rock avalanche moved along a narrow tributary gorge (laterally confined type according to Shaller [56]) before entering a wide flood-plane of the main river, where confinements disappear abruptly.

For example, Kazarah, Satpura Lake-Skardu, Ghoro Ghoh and some other rock avalanches described by Hewitt [27] form fan-shaped or pancake-shaped tongues when they enter wide flood-planes of the Indus, Gilgit and Hunza Rivers. The same occurred at Sherman Glacier [41]. A different effect can be observed at the Chongsu, Southern Karakungey (see figure 5), and especially at the Chaartash-2 [66] sites, where, after entering wide plains within intermountain depressions, the debris continued to move forward, forming monodirectional rock avalanches with little or no widening.

It seems that the width-to-length ratio of the debris apron, which corresponds to the extent of lateral widening of a rockslide deposit, strongly depends on the shear strength of the basement along which debris moves. Most of the monodirectional rock avalanches are in arid environments. Besides the above mentioned cases, other examples are the Blackhawk rock avalanche in the Californian desert [32, 61], the Sierra Laguna Blanca and Sierra Aconquija rock avalanches in the arid zone of Argentina [23, 25], the Chaartash-3 rock avalanche in the Central Tien Shan (see figure 7) [66]. Similar morphology can be seen in some Martial rockslides [56], which most probably, occurred in dry, waterless conditions.

In contrast, pancake-shaped and fan-shaped types are usually formed when rockslides descend onto saturated flood planes. Examples are the Atdjailau rock avalanche in Tien Shan (see figure 7), the above mentioned Karakoram cases, or on gently inclined ice surface such as Sherman Glacier event [41]. Of course there are exceptions, but in the majority of cases such correlation seems to be correct.

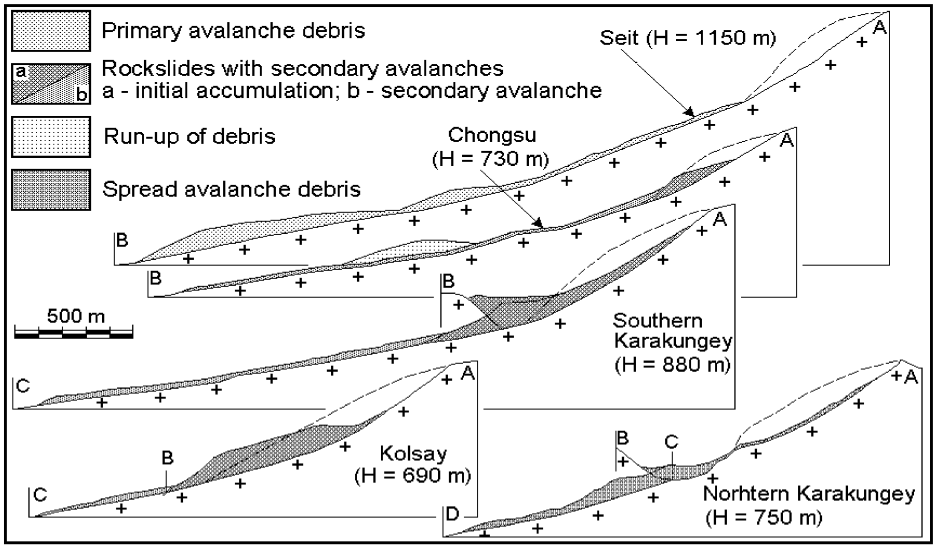

Figure 6. Schematic profiles of rock avalanches shown on figure 5 (after [65]). H – height from the head of the scar to the avalanche toe.

The low shear strength of the saturated gravel on wide, flat flood plains of post-glacial valleys, as well as the low strength of ice and snow on glaciers create favourable conditions for the debris to spread in all possible directions, both forward and lateral. This effect was analysed by Sassa and his colleagues [53]. A low basal shear strength could be the main cause of the 'finger deposition' described at the Marquartstein and Altenau rockslides in Bavarian Alps by Poschinger [49]. In contrast, dry soil and gravel in the arid zones are much stronger and their shearing requires more intensive load provided only by the forward motion. In many cases, intense lateral spreading of debris started long before its collision (if any) with some obstacle or at an opposing slope. This supports the assumption that the presence or absence of lateral spreading of a rockslide deposits is governed mainly by processes acting during debris motion, rather than by its topographic confinement as was suggested by Hewitt [29].

As mentioned above, it has been shown that the H/L ratio is not the most adequate parameter with which to characterise rock avalanche mobility [39], especially where the debris is spread over an unconfined surface. It seems that Debris Apron Area (DAA) is a better reflection of real relationships. Since friction acts over the entire basal surface, it should be proportional the square of the linear dimension. It is evident that rock avalanches with similar parameters of initial failure that move over unconfined surface and form wide aprons are more mobile then those that move strictly ahead (Figure 9).

For unconfined rock avalanches use of several additional parameters characterising lateral spreading of debris can be proposed: $W_{max}/W_{initial}$ or $(W_{max}/W_{initial})/L$ or $(W_{max}-W_{initial})/L$. Following Korchevsky and Muratova [37] I suggest that the formal planimetric width of the debris apron at the middle of debris runout as suggested by Nico-

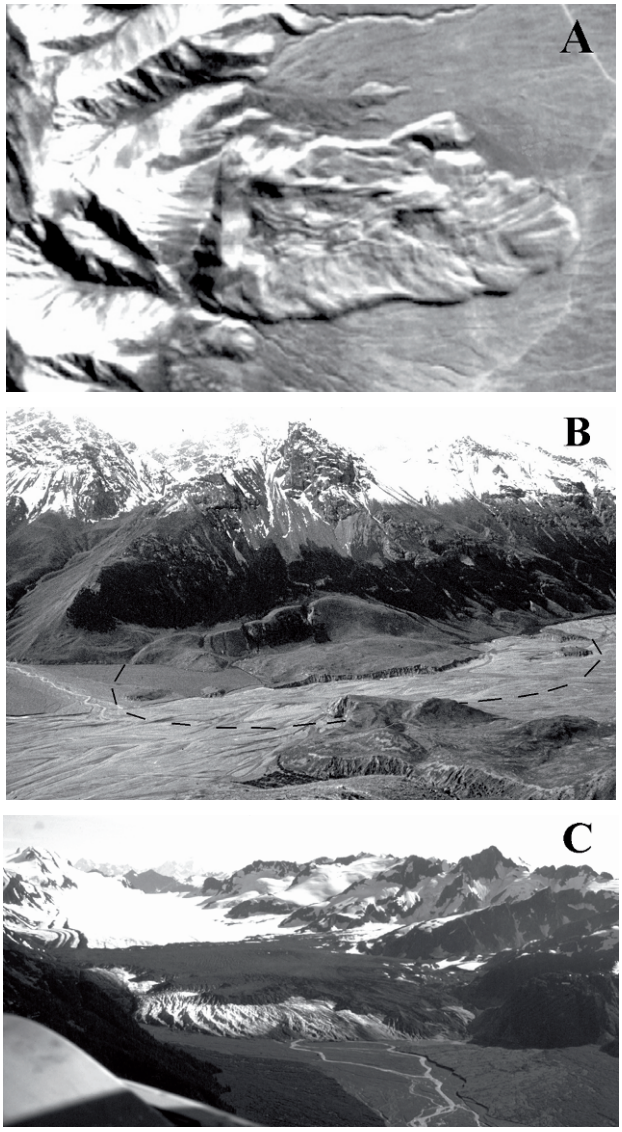

Figure 7. Debris distribution typical of unconfined rock avalanches. A - Chaartash-3 rock avalanche in Paleozoic granite, about 300×10^6 m^3 in volume, in the Central Tien Shan (41.24º N, 74º E). Part of high-resolution space photo. Rock avalanche moved forward across an unconfined surface (dry gravel bottom of the intermountain depression) about 3.5 kilometres with little lateral spreading. Good example of monodirectional rock avalanche. B - Atdjailau rock avalanche in Paleozoic limestone, about 50×10^6 m^3 in volume, in the Eastern Tien Shan (42.15º N, 79.45º E). Rock avalanche spread over unconfined surface (saturated gravel and pebble flood plane of the Inylchek river) and formed a 'pancake-shaped' apron 1200 m in a radius and 10-50 m thick. C - Sherman Glacier rock avalanche, Alaska, 1964, 27×10^6 m^3 in volume (photograph courtesy of M. McSaveney). Famous example of a rock avalanche that spread over a glacier forming a fan-shaped apron. In cases B and C the mechanical properties of underlying surface determined a low basal shear strength.

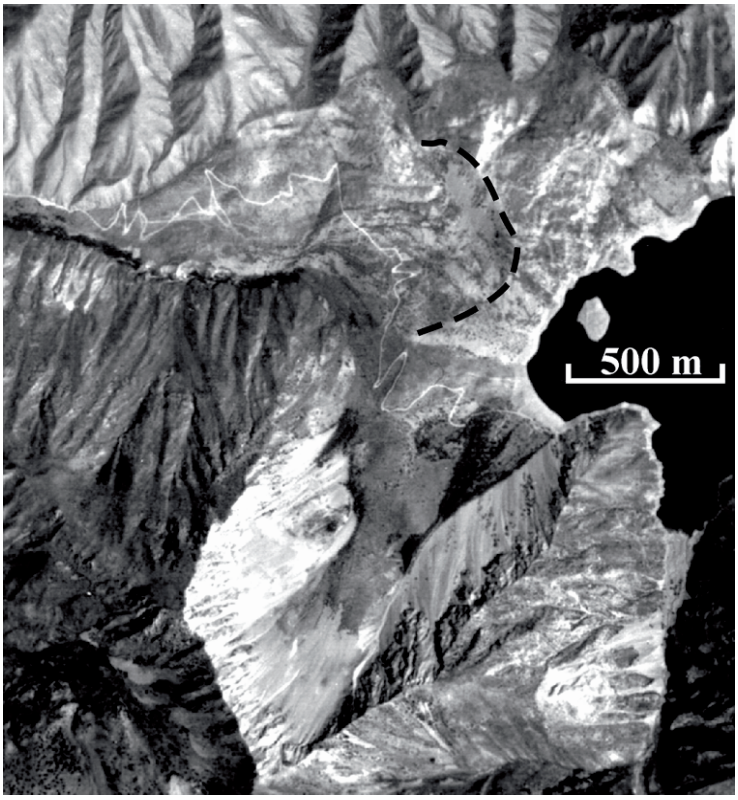

Figure 8. The Karasu Lake rockslide (41.9º N, 73.22º E) 2.5×10^8 m^3 in volume. Part of high-resolution space photo. Secondary scar from which debris spread downstream is marked by dashed line.

letti and Sorriso-Valvo [47] not be used. The width of the mouth of the scar ($W_{initial}$ on figure 9), seems to be more a realistic parameter.

4.5. MICRO-RELIEF OF THE DEPOSITS

Besides the overall morphology of rockslides and rock avalanches described above, the micro-morphology of deposits is very informative in reconstructing debris motion. It can be used as a further classification criterion. Several distinct types of micro-relief can be recognised. Parallel or fan-shaped diverging levees and furrows indicating 'laminar flow' of debris (see the frontal part of the Chaartash-3 rock avalanche shown on figure 7-A). Transverse levees described, for example, by Eppler et al. [12] and McSaveney [41], which are interpreted as the result of longitudinal compression in the moving rock avalanche (as was pointed out by Murge [46] "arcuate ridges and furrows signify only that the deposit moved but do not necessarily imply that the deposit was wet or dry or that it moved rapidly or slowly"). Hummocky relief typical of rock avalanches, with mollards – conical hills up to several meters high, indicate the opposite mode of defor-

mation – intensive tensile strain in the upper part of the moving debris [11, 32, 62] (see, for example the central part of the rock avalanche shown on figure 11).

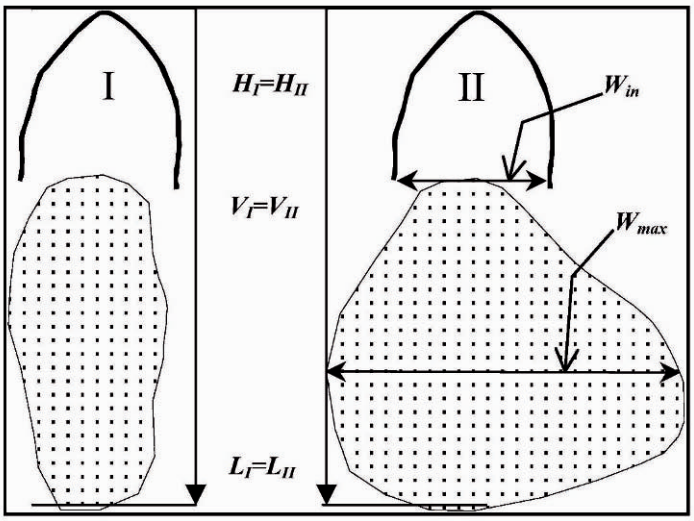

Figure 9. Comparison of rockslides with similar basic parameters (V, H, L) but with significantly different debris apron area (DAA).

5. Gradations in Morphological and Structural Parameters

The above comparative analysis allows us to select rockslides and rock avalanches that represent different stages of a successively developing process. This can be illustrated either by a set of case studies, or by a single event with significant differences of some parameters one different parts of its debris apron.

The first of these possibilities is shown by the Usoi→Karasu Lake→ Southern Kara-Kungei series of rockslides, that feature different involvement of debris in avalanche-like motion, and increasing mobility of secondary avalanches accompanying these blockages (compare figures 10 and 8).

A significant difference in micro-morphological features corresponding to an abrupt change in deformational pattern and dynamics of debris motion can be observed on the Bayan-Nur rock avalanche in Mongolian Altai (Figure 11). There are several distinct zones in its deposits. The internal zone has a hummocky relief formed by numerous mollards, indicating extension. The outer lobate zone, with diverging levees inside each lobe, was formed by parallel 'flow' of portions of the debris. The western part of this rock avalanche is bounded by a well expressed frontal rim with steep slope indicating progressive debris accumulation in front of the moving debris, and an abrupt halt in motion. A huge debris accumulation typical of secondary or spread avalanches can be recognised at the foot of the scar.

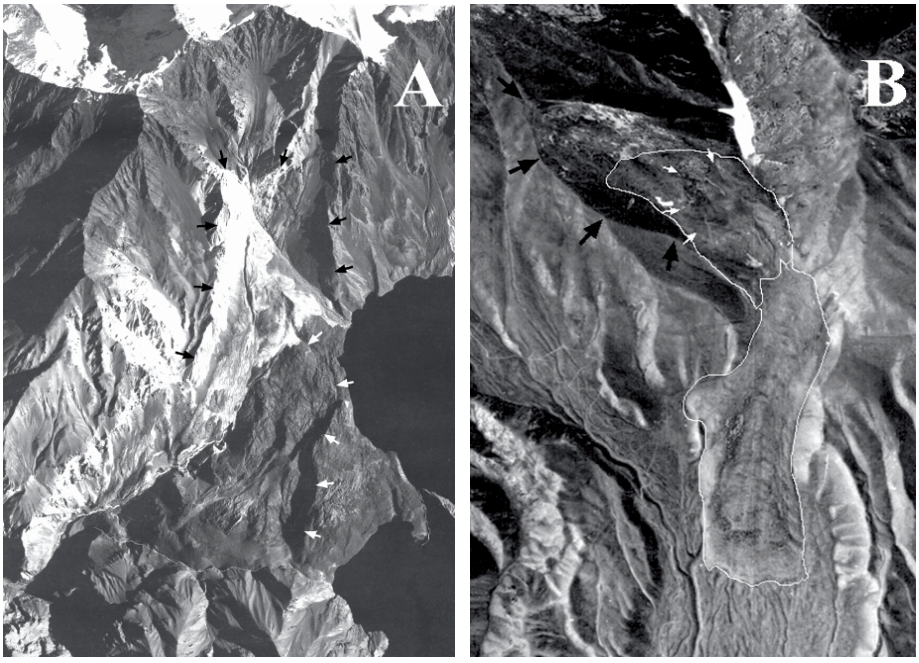

Figure 10. Rockslides with different extent of secondary avalanches' development. Black arrows mark initial scars, white arrows – secondary scars. A - the Usoi rockslide 2.2×10^9 m^3 in volume. A clear arcuate escarpment marks the secondary slide on the downstream slope of the blockage, which did not converted into avalanche-like motion; B - the Southern Karakungey rockslide 20×10^6 m^3 in volume (see also figure 5-D). Its secondary scar marks the source zone of avalanche, which involved about halve of the total debris volume. See also Karasu Lake rockslide (figure 8) which represents an intermediate stage of secondary avalanche formation.

6 Discussion

The universal features described in the above case studies, and the classification criteria that reflect patterns within different groups of rockslides and rock avalanches, are significantly interconnected. Their joint analysis allows the kinematic and dynamic characteristics of debris motion to be reconstructed.

For example, the overrunning and overthrusting of the frontal parts of the debris by the proximal portions, resulting in the formation of 'multi-layered' rockslide deposits must lead to an increase in thickness of the moving debris, and, thus, to an additional overburden pressure on the lower units. This can, in turn, intensify the processes that lead to debris comminution and crushing.

For example, according to Melosh's [42-45] acoustic fluidisation model, intense elastic vibrations arise in the collapsing rock mass and create local pressure fluctuations. Originally this model was developed to explain the abnormal mobility of large rockslideshe postulates that shearing occurs locally where normal stress in any limited portion

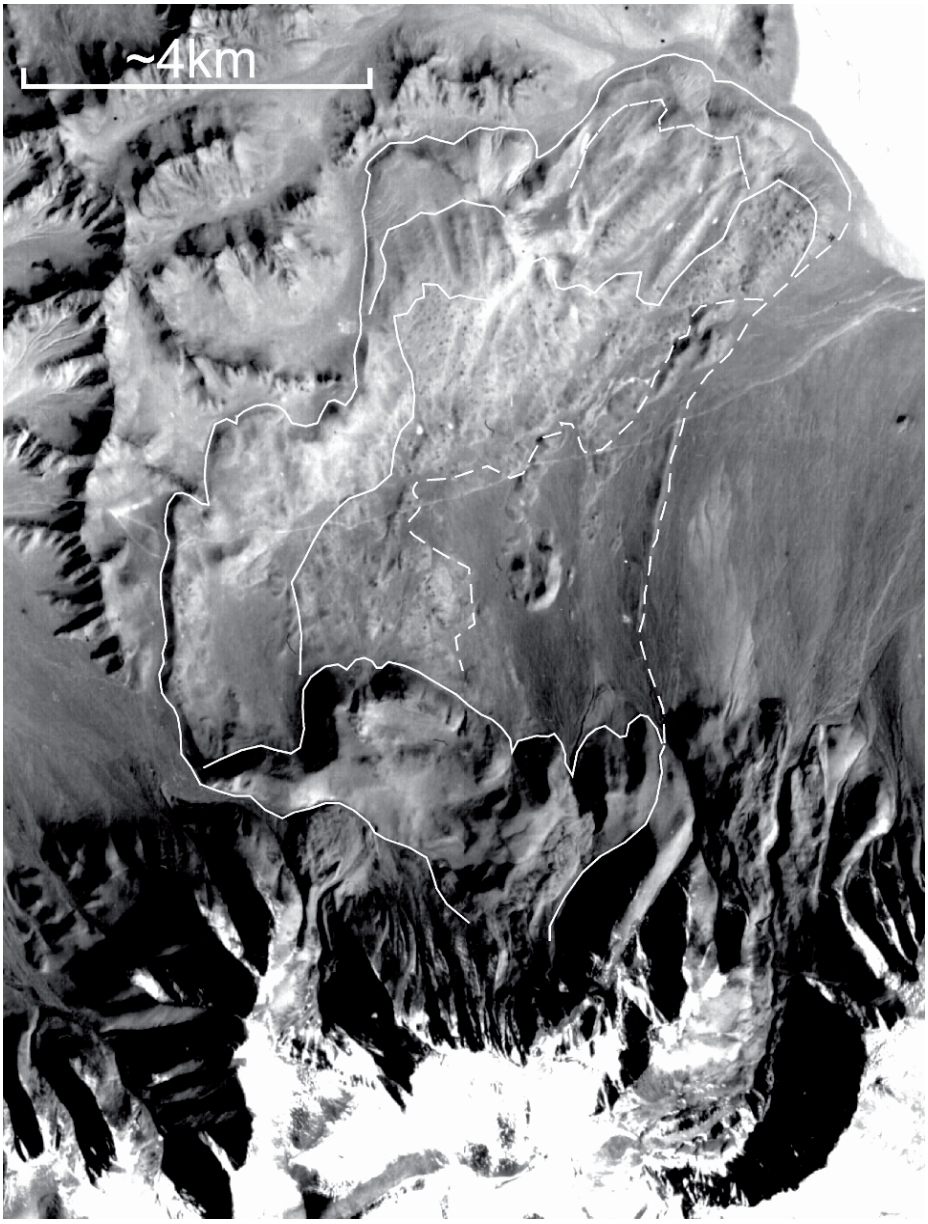

Figure 11. Giant Bayan-Nur rock avalanche in Mongolian Altai (48.85º N, 90.77º E) featuring gradation in its debris apron morphology. The outer limit of debris and boundaries between zones with different micro-relief are highlighted by white lines. Boundaries in the eastern part of the debris apron where the rock avalanche has been eroded or covered by the deposits of debris flows are shown as dashed lines.

of debris decreases due to acoustic pressure fluctuations. However, we can extend it, taking into consideration that local normal stress value depends on the overlying debris thickness. Melosh noted that when pressure fluctuations exceed the overburden pressure, local failure within the rock mass should occur [44]. After debris overthrusting, when the overburden pressure increases abruptly, the probability that local stress will exceed the rock's strength will increase, and the probability of debris shattering should increase too [63]. This should be most effective when a high dam is formed, since high overburden pressure is maintained in it lower part until the motion halts. Although the validity of the acoustic-fluidisation model is questionable, its predicted effects match with observable features.

On the other hand, the more shattered the debris becomes, the more its characteristics and behaviour should correspond to those of a liquid. In particular, it should undergo intensive thinning due to the weight of the overlaying material. Due to the likely abrupt change of mechanical properties between the lower (shattered) and upper (blocky) zones (see figure 1), the thinning and lateral spreading of the lower zone must create tension in the upper zone. Such tension is confirmed by presence of mollards and clastic dikes filled by material from the lower 'layer' [32].

Thinning should significantly increase debris velocity according to the initial and final thickness ratio and, thus, must effect rock avalanche runout. If the volume density of debris after main crushing have occurred is assumed as constant, volume (V) of any unit that experience such thinning should be constant too. It can be exemplified by simple equations:

$$V=kr_0^2\times h_0 = kr_f^2\times h_f \quad (1)$$

where r_0 is the initial linear dimension; r_f – the final linear dimension; h_0 - the initial thickness; h_f – the final thickness, and k is the coupling coefficient between linear dimension and shape of the analysed unit (for example, if it is a cylinder than $k=\pi$).

$$r_f=r_0(h_0/h_f)^{1/2} \quad (2)$$

$$\Delta r=(r_f - r_0)=r_0((h_0/h_f)^{1/2} - 1) \quad (3)$$

where Δr is the increase in the linear dimension. Thus, the additional velocity of the debris due to its thinning should be proportional to the initial linear dimension r_0 and to the h_0/h_f ratio:

$$\Delta r/t = r_0((h_0/h_f)^{1/2} - 1)/t \quad (4)$$

where 't' is the duration of the process. If thinning depends on the comminution of the lower part of debris, $(h_0/h_f)^{1/2}$ increases and additional velocity becomes significant when material is highly crushed. In fact, due to the dilation associated with continuing fragmentation (M. McSaveney, Personal Communication, 2002), the debris volume must increase, therefore the effect of thinning on acceleration of the debris should be even sharper.

Other consequence is that acceleration of moving debris due to its thinning should be higher in those directions, where $\mathbf{r}_0$ is larger. The initial shape of moving rock-debris mass depends on topographic constraints and, as shown in section 4.4, on the shear strength at the underlying surface, especially for unconfined events. In so far as inten-

sive shattering takes place practically in all cases of large-scale massive slope failures, thinning should significantly increase rock avalanche runout.

7. Conclusions

Systematisation and classification of the different features typical of rockslide and rock avalanche deposits enables a better understanding of the interrelations between their shape, morphology and internal structure. Comprehensive analysis of further case studies will allow more features typical of massive rock slope failures to be taken into consideration and will help to develop universal, non-contradictory mechanical models for the formation and motion of rockslides and rock avalanches. These then may be applied to different engineering and emergency uses, such as the construction of blast fill dams [3, 37, 38], stability of rockslide-dammed lakes [6], and hazard assessment in rockslide-prone mountainous regions.

Acknowledgements

I want to express my gratitude to Mauri McSaveney, Patrick Wassmer, Kenneth Hewitt, Andreas von Poschinger, Steve Evans, Reginald Hermanns and Gabriele Scarascia Mugnozza for useful discussions.

References

1. Abdrakhmatov, K., and Strom, A.L. (2003) Dissected rockslide and rock avalanche deposits; Tien Shan, Kyrgyzstan (this volume).
2. Abele, G. (1974) *Bergsturze in den Alpen*, Wissensch, Alpenvereinshefte, Munchen H. 25.
3. Adushkin, V.V. (2000) About initiation of natural creative processes by explosions, *Combustion, Explosion, and Shock Waves* **36**, No 6, 21-30.
4. Avdeev, V.A., Nartov, S.V., Baljinniam, I., Monhoo, D., and Erdenbileg, B. (1989). Tsambagarav earthquake of July 23, 1988, *Geology and Geophysics*, No 11, 118-124. (in Russian)
5. Campbell, C.S. (1989) Self-lubrication for long runout landslides, *J. Geology* **97**, 635-665.
6. Costa, J.E., and Schuster, R.L. (1988) The formation and failure of natural dams, *Geol. Soc. Am. Bull.* **100**, 1054-1068.
7. Couture, R., Antoine, P., Locat, J., Hadjigeorgiou, J., Evans, S.G., Brugnot G. (1997) Quatre cas d'avalanches rocheuses dans les Alpes françaises, *Can. Geotechnical J.* **34**, 102-119.
8. Davies, T.R. (1982) Spreading of rock avalanche debris by mechanical fluidisation, *Rock Mechanics* **15**, 9-24.
9. Davies, T.R., and McSaveney, M.J. (1999) Runout of dry granular avalanches *Can. Geotechnical J.* **36**, 313-320.
10. Davies, T.R., and McSaveney, M.J. (2002) Dynamic simulation of the motion of fragmenting rock avalanches, *Can. Geotechnical J.* **39***,* 789-798.
11. Eisbacher, G.H. (1979) Cliff collapse and rock avalanches (sturzstroms) in the Mackenzie Mountains, northwestern Canada, *Can. Geotechnical J.* **16**, 309–334.
12. Eppler, D.B., Fink, J., and Fletcher, R. (1987) Rheologic properties and kinematics of emplacement of the Chaos Jumbles rockfall avalanche, Lassen Volcaic National Park, California, *J. Geophys. Res.* **B95,** 3623-3633.
13. Erismann, T.H. (1979) Mechanisms of large landslides, *Rock Mechanics* **12**, 15-46.
14. Erismann, T.H. (1986) Flowing, rolling, bouncing, sliding: synopsis of basic mechanisms, *Acta Mechanica* **64**, 101-110.

15. Ermini, L., and Casagli, N. (2002) Criteria for a preliminary assessment of landslide dams evolution, in Ribář, Stemberk and Wagner (Eds), in *Landslides*, *Proc. of the First European Conf. on Landslides, Prague, June 24-24, 2002*. Swets & Zeitlinger, Lisse, 157-162.
16. Evans, S.G., Hungr O., and Enegren E.G. (1994) The Avalanche Lake rock avalanche, Mackenzie Mountains, Northwest Territories, Canada: description, dating and dynamics, *Can. Geotechnical J.* **31**, 749-768.
17. Fedorenko, V.S., Nikulin, F.V., Kalinin, E.V., and Lipilin V.I. (1979) Mechanism of large rockslides' displacement, *Engineering Geology* No 6, 30-46 (in Russian).
18. Grigorian, S.S. (1979) New friction law and mechanism of large-scale rockfalls and landslides, *Proceedings of Academy of Sciences of USSR* **244**, 846-849 (in Russian).
19. Habib, P. (1975) Production of gaseous pore pressure during rock slides, *Rock Mechanics*, **7**, 193-197.
20. Harrison, J.V. and Falcon, N.L. (1937) The Saidmarreh landslip, southern Iran, *J. Geography* **89,** 42-47.
21. Heim, A. (1882) Der Bergsturz von Elm,. *Z. der Deutschen Geologishen Gesellschaft* **34**, 74-115.
22. Heim, A. (1932) *Der Bergsturz und Menschenleben*, Fretz und Wasmuth, Zurich.
23. Hermanns, R. L., Strecker M.R. (1999) Structural and lithological controls on large Quaternary rock avalanches (sturzstroms) in arid northwestern Argentina, *Geol. Soc. Am. Bull.* **111**, 934-948.
24. Hermanns, R. L., Trauth, M.H., Niedermann, S., McWilliams, M., and Strecker M.R. (2000) Tephrochronologic constraints on temporal distribution of large landslides in northwest Argentina, *J. Geology* **108**, 35-52.
25. Hermanns, R. L., Niedermann, S., Garsia, A.V., Gomes J.S., and Strecker M.R. (2001) Neotectonics and catasrophic failure of mountain fronts in the southern intra-Andean Plateau, Argentina, *Geology* **29**, 619-623.
26. Hewitt, K. (1988) Catastrophic landslide deposits in the Karakoram Himalaya, *Science* **242**, 64-67.
27. Hewitt, K. (1999) Quaternary moraines vs catastrophic rock avalanches in the Karakoram Himalaya, Northern Pakistan, *Quaternay Research* **51**, 220-237.
28. Hewitt, K. (2001a) Catastrophic rockslides and the geomorphology of the Hunza and Gilgit river valleys, Karakoram Himalaya, *Erdkunde* **55**, 72-93.
29. Hewitt, K. (2002) Styles of rock avalanche depositional complex in very rugged terrain, Karakoram Himalaya, Pakistan, in Evans, S.G. and DeGraff, J.V. (eds.), Catastrophic Landslides: effects, occurrence and mechanisms. Reviews in Engineering Geology XV, Boulder, Colorado.
30. Hsu, K.J. (1975) Catastrophic debris streams generated by rockfalls, *Geol. Soc. Am. Bull*. **86**,129-140.
31. Hsu, K.J. (1978) Albert Heim: observations on landslides and relevance to modern interpretations, in B. Voight (Ed.), *Rockslides and Avalanches*, **1**, *Natural Phenomena*, Amsterdam: Elsevier, 71-93..
32. Johnson, B. (1978) Blackhawk landslide, California, U.S.A, in B. Voight (Ed.), *Rockslides and Avalanches*, **1**, *Natural Phenomena*, Amsterdam: Elsevier,. 481-504.
33. Kent, P.E. (1966) The transport mechanism in catastrophic rockfalls, *J. of Geology* **74**, 79-83.
34. Kilburn, C.R.J., Søremsen, S-A. (1998) Runout length of sturzstroms: the control of initial conditions and of fragment dynamics, *J. Geophys. Res.* **103**, No B8, 17877-17884.
35. Kobayashi, Y. (1993) A hypothesis for reduced resistance in large landslides, in *Safety and Environmental Issues in Rock Engineering,* Proc. of the ISRM Int. Symp. Lisboa, June 21-24, 1993 **1**, Balkema Rotterdam, pp. 835-839.
36. Kobayashi, Y. (1997). Long runout landslides riding on basal guided wave, in Marinos, Koukis, Tsiambaos & Stoumaras (Eds.) *Engineering Geology and the environment*, Balkema, Rotterdam, 761-766.
37. Korchevsky, V.F., and Muratova, M.H. (1991) Construction of dams by collapse, *Hydrotechnical Construction,* No 3, 6-11 (in Russian).
38. Korchevsky, V.F. and Petrov, G.N. (1989) *Designing and investigation of blastfill dams,* Energoatomisdat, Moscow, (in Russian).
39. Legros, F. (2002) The mobility of long-runout landslides, *Engineering Geology* **63**, 301-331.
40. Li, Tianchi (1983) A mathematical model for predicting the extent of a major rockfall, *Z. für Geomorphologie N.F.,* **27**, 473-482.
41. McSaveney, M.J. (1978) Sherman glacier rock avalanche, in B. Voight (Ed.), *Rockslides and Avalanches* **1**, *Natural Phenomena*, Amsterdam, Elsevier, 197-258.
42. Melosh, H.J. (1979) Acoustic fluidization: a new geologic process? *J. Geophys. Res.* **84**, 7513-7520.
43. Melosh, H.J. (1983) Acoustic fluidisation, *American Scientist* **71**, 158-168.
44. Melosh, H.J. (1986) The physics of very large landslides, *Acta Mechanica* **64**, 89-99.

45. Melosh, H.J. (1990) Giant rock avalanches, *Nature* **348**, 483-484.
46. Murge, M.R. (1965) Rockfall-avalanche and rockslide-avalanche deposits at Sawtooth Ridge, Montana. *Geol. Soc. Am. Bull.* **76**, 1003-1014.
47. Nicoletti, P.G. and Sorriso-Valvo M. (1991) Geomorphic controls of the shape and mobility of rock avalanches, *Geol. Soc. Am. Bull.* **103**, 1365-1373.
48. Ostroumov, A.V. (1986) Mechanism of friction in rockfall flows, in *Problems of soil thermomechanics*, Moscow State University, 37-48. (in Russian).
49. Poschinger, A. von (1994) Some special aspects of the "impact" of a landslide on the valley floor, *Landslide News*, No 8, 26-28.
50. Potapov A.V. (1991) *Numerical modelling of the nonstationary geomechanical processes with low internal friction*, Ph.D. Thesis, Institute of Geospheres Dynamics, RAS, (in Russian).
51. Rezvoi, D.P., Rezvoi, P.D. (1969) Lake that vanished …, *Priroda (Nature)*, No 7, 81-83. (in Russian).
52. Richter, Ch. F. (1958) *Elementary Seismology*. W.H. Freeman and Company, San Fransisco.
53. Sassa, K., Fukuoka H., Lee, J-H., Shoaei Z., Zhang, D., Xie, Z., Zeng, S, Cao, B. (1994) Prediction of landslide motion based on the measurement of geotechnical parameters, in: *Developement of a new Cyclic Loading Ring Shear Apparatus to study earthquake-induced-landslides*. Report for Grant-in-Aid for Developmental Scientific Research by the Ministry of Education, Science and Culture, Japan (Project No 03556021), DPRI, Kyoto, 72-106.
54. Scarascia Mugnozza, G., Fasani, G.B., Esposito, C., and Evans S.G. (2003) Prehistoric rock avalanches, mountain slope deformations and hazard conditions in the Maiella Massif (Central Italy), this volume.
55. Schneider, J.-L., Wassmer, P., Ledésert, B. (1999) La fabrique interne des dépôts du sturzstrom de Flims (Alpes suises): caractéristiques et implications sur les méchanismes de transport, *C.P. Acad. Sci. Paris. Earth & Plan. Sci.* **328**, 607-613.
56. Shaller, P.J. (1991) *Analysis and implications of large Martian and Terrestrial landslides*, Ph.D. Thesis, California Institute of Technology.
57. Sheko, A.I., and Lekhatinov, A.M. (1970) Present date state of the Usoy blockadge and tasks of future investigations, in *Materials of Scientific-Technical Meeting on the Methodical Problems of Mud Flows, Rockfalls and Landslides Investigation and Forecast*, Dushanbe, Donish, 219-223. (in Russian).
58. Sheidegger, A.E. (1973) On the prediction of the reach and velocity of catastrophic landslides, *Rock Mechanics* **5**, 231-236.
59. Shemiakin, E.I. (1993) On the mobility of large landslides, *Proceedings of Russian Academy of Sciences* **331**, 742-744 (in Russian).
60. Shoaei, Z. and Ghayoumian, J. (2000) Seimareh landslide, Western Iran, one of the World's largest complex landslides, *Landslide News*, No 13, 23-27.
61. Shreve R.L. (1968) The Blackhawk landslide, Geological Society of America Special Paper. N 108.
62. Solonenko, V.P. (1970) Scars on the Earth's face. *Priroda (Nature)*, No 9, 17-25. (in Russian).
63. Strom, A.L. (1994) Mechanism of stratification and abnormal crushing of rockslide deposits, in *Proc. 7th International IAEG Congress* **3**, Rotterdam, Balkema, 1287-1295.
64. Strom, A.L. (1994) Formation of structure of large rockslide deposits, *Geoecology, Engineering Geology, Hydrogeology, Geocryology,* No 5, 64-77 (in Russian).
65. Strom, A.L. (1996) Some morphological types of long-runout rockslides: effect of the relief on their mechanism and on the rockslide deposits distribution, in K. Senneset (Ed.) *Landslides*. Proc. of the Seventh International Symposium on Landslides, 1996, Trondheim, Norway, Rotterdam, Balkema, 1977-1982.
66. Strom, A.L. (1998) Giant ancient rockslides and rock avalanches in the Tien Shan Mountains, Kyrgyzstan, *Landslide News*, No 11, 20-23.
67. Van Gassen, W., and Cruden, D.M. (1989) Momentum transfer and friction in the debris of rock avalanches, *Can. Geotechnical J.* **26**, 623 - 628.
68. Wassmer, P., Schneider, J.-L., and Pollet, N. (2002) Internal structure of huge Mass Movements: a key for a better understanding of long runout. The multy-slab theoretical model, in *Proc. Int. Symp. Landslide Risk Mitigation and Protection of Cultural and Natural Heritage*. 21-25 Jan., Kyoto University, Kyoto, 97-107.
69. Watson, R.A., and Wright Jr., H.E. (1969) The Saidmarreh landslide, Iran, *Geol. Soc. Am. Special Paper* **123**, 115-139.